HHS Public Access

Author manuscript

J Pediatr Surg. Author manuscript; available in PMC 2022 February 01.

Published in final edited form as:

J Pediatr Surg. 2021 February ; 56(2): 250–256. doi:10.1016/j.jpedsurg.2020.04.002.

Pan-enteric neuropathy and dysmotility are present in a mouse model of short-segment Hirschsprung disease and may contribute to post-pullthrough morbidity

Sukhada Bhave, **Emily Arciero**, **Corey Baker**, **Wing Lam Ho**, **Richard A. Guyer**, **Ryo Hotta**, **Allan M. Goldstein***

Department of Pediatric Surgery, Massachusetts General Hospital, Harvard Medical School, Boston, MA

Abstract

Purpose—Hirschsprung disease (HSCR) is characterized by distal intestinal aganglionosis. While surgery is lifesaving, gastrointestinal (GI) motility disorders persist in many patients. Our objective was to determine whether enteric nervous system (ENS) abnormalities exist in the ganglionated portions of the GI tract far proximal to the aganglionic region and whether these are associated with GI dysmotility.

Methods—Using *Ednrb*-null mice, a model of HSCR, immunohistochemical analysis was performed to evaluate quantitatively ENS structure in proximal colon, small intestine, and stomach. Gastric emptying and intestinal transit were measured *in vivo* and small and large bowel contractility were assessed by spatiotemporal mapping *ex vivo*.

Results—Proximal colon of HSCR mice had smaller ganglia and decreased neuronal fiber density, along with a marked reduction in migrating motor complexes. The distal small intestine exhibited significantly fewer ganglia and decreased neuronal fiber density, and this was associated with delayed small intestinal transit time. Finally, in the stomach of HSCR mice, enteric neuronal packing density was increased and gastric emptying was faster.

Conclusions—ENS abnormalities and motility defects are present throughout the ganglionated portions of the GI tract in *Ednrb*-deficient mice. This may explain the GI morbidity that often occurs following pull-through surgery for HSCR.

Keywords

Hirschsprung disease; enteric nervous system; dysmotility; *Ednrb*

*Corresponding Author: Allan M. Goldstein, MD, Dept. of Pediatric Surgery, Massachusetts General Hospital, 55 Fruit St, Warren 1151 Boston, MA 02114, agoldstein@partners.org.

1. Introduction

The enteric nervous system (ENS) is an extensive network of neurons and glia within the wall of the gastrointestinal (GI) tract that is critically important for regulating gut motility and other aspects of GI function [1]. The ENS arises from enteric neural crest-derived cells that migrate from the neural tube to colonize the intestine during development [2]. In Hirschsprung disease (HSCR), a congenital disorder that affects 1 in 5000 live births [3], the migrating cells fail to populate variable lengths of distal bowel, resulting in distal intestinal aganglionosis. The uncolonized bowel remains contracted and functionally obstructed. The only effective treatment is surgical resection of the diseased bowel.

Despite resection of the aganglionic segment, HSCR patients often suffer from persistent GI problems, including constipation and fecal incontinence, which significantly impacts quality of life [4]. These issues may arise from technical factors related to the operation [5], but there is considerable evidence that functional abnormalities exist proximal to the aganglionic segment. Manometric studies have shown altered contractility and duration of contractions in the esophagus and duodenum of patients with HSCR when compared to healthy controls [6–8]. Radiographic studies have revealed slower gastric emptying and longer colonic transit times in patients with HSCR [9, 10]. These studies suggest the presence of functional ENS perturbations remote from the grossly diseased region.

Mouse models of HSCR have confirmed the presence of abnormalities in the ganglionated bowel. For example, *Ednrb*$^{-/-}$ mice possess decreased neuronal density and increased neuronal size in the ganglionated colon [11]. Both mice and humans with HSCR exhibit an imbalance of neuronal subtypes in the ganglionated proximal colon, with an overabundance of nitrergic innervation and a deficit of cholinergic innervation [12]. However, characterization of the ENS in HSCR has been restricted to the colon. We therefore undertook an examination of the ganglionated colon, small intestine, and stomach in *Ednrb*-deficient mice, a commonly utilized model of short-segment HSCR, and describe alterations of both ENS structure and intestinal motor function throughout the length of the GI tract. Identifying these abnormalities will have important clinical implications for our understanding, diagnosis, and treatment of patients with GI complications following pullthrough surgery.

2. Methods

Animals

All the animal protocols were conducted in accordance with the procedures reviewed and approved by the Institutional Animal Care and Use Committee at Massachusetts General Hospital. Five mice were housed per cage in 12/12 light–dark cycle. Access to food and water was available *ad libitum* throughout the experiments. Mice used for all the experiments were three weeks old. Each experimental group consisted of both male and female mice.

Ednrb^{tm1Ywa} mice on a hybrid C57BL/6J-129Sv background were purchased from Jackson Laboratory (Bar Harbor, ME; Stock Number 003295). *Ednrb*$^{-/-}$ homozygous pups were

identified by a white coat color and exhibit distal aganglionosis [13]. Mice were genotyped using polymerase chain reaction (PCR) to distinguish between wild type *Ednrb*$^{+/+}$ (annotated as WT) (500 bp), heterozygous *Ednrb*$^{+/-}$ (300 and 500 bp), and knockout *Ednrb*$^{-/-}$ littermates (annotated as KO) [14]. Primer pairs used for *Ednrb* were: Forward 5`-GATGAACCTGC-3`, Mutant Forward 5`-ATAGATTCGCC-3` and Reverse 5`-CATGGTCTTGT-3`.

Immunohistochemistry

Immunohistochemistry was performed on proximal colon, distal small intestine, and stomach, from WT and KO mice, as previously described [12]. Whole mount preparations of the longitudinal muscle myenteric plexus (LMMP) and full-thickness gut samples were fixed in 4% paraformaldehyde. Tissue samples were embedded in 15% sucrose containing 7.5% gelatin for cryosectioning. Frozen sections were cut at 12 μm thickness with a Leica CM3050S cryostat (Leica, Buffalo Grove, IL). LMMP preparations and tissue cryosections were permeabilized with 0.1% Triton X-100 and blocked with 10% donkey serum. Primary antibodies were diluted in 10% donkey serum and included mouse anti-neuronal class III conjugated β-tubulin (Tuj1; 1:400; Covance, Dedham, USA), human anti-HuC/D (Anna1, 1:16000, kindly gifted by Lennon lab), and rabbit anti-Nestin (NES, 1:200, Abcam, Cambridge, UK). Secondary antibodies included anti-rabbit IgG (1:500; Alexa Fluor 488; Fisher Scientific Life Technologies) and antihuman IgG (1:200, Alexa Fluor 594; Fisher Scientific Life Technologies). Cell nuclei were stained with DAPI (Vector Labs, Burlingame, CA) and mounted with aquapoly/mount (Fisher Scientific Polysciences Inc). Images were taken using Nikon A1R laser scanning confocal microscope (Nikon Instruments, Melville, NY).

Morphometric analysis

ENS architecture in WT and KO mice (n=3–7 mice per group) was morphometrically quantified using wholemount LMMP preparations and cross sections of the proximal colon, distal small intestine, and stomach. High-power images of the LMMP preparations and tissue cross-sections were taken at 10x and 20x magnification using a Nikon A1R-A1 confocal microscope. Image acquisition was carried out with NIS-Elements imaging software (Nikon). Images were analyzed using the Image J software. From LMMP preparations, Hu+ neuronal cell bodies and Tuj1+ neuronal fibers were analyzed per high-power field from 3 images per animal. Neuronal packing density was calculated as the number of Hu+ neuronal cell bodies per area of the ganglia. Neuronal packing was analyzed for every ganglia from 3 fields per animal. High-power images of tissue cross sections were used to analyze the number of ganglia per field and size per ganglia, where measurements were made from 3 images per animal and the size of each ganglia was measured in the field.

Ex vivo measurement of GI motility

Contractile movement of isolated distal small intestine and colon was analyzed *ex vivo.* After euthanizing the mice, whole colon and the distal-most 6-cm piece of ileum was excised immediately and placed in an illuminated organ bath continuously perfused with Krebs solution at 36.5 ± 0.5 °C and bubbled with carbogen gas (95% O_2/5% CO_2). Tissue was anchored with pins at the anal and oral end. Intestinal motility was recorded from each

mouse for 30 minutes using Gastrointestinal Motility Monitoring system (GIMM; Med-Associates, St. Albans, VT, USA). Video recordings from each animal were used to generate kymographs of intestinal contractions using the GIMM software [15]. Frequency, length, and velocity of colonic migrating motor complexes (CMMCs) were analyzed from the kymographs for the proximal colon using the GIMM processor plugin (Image J) [16]. For the distal small intestine, the frequency and amplitude of segmentation contractions was measured. Contraction profile over a given period of time was represented as area under the curve (AUC). Five regions of interest (ROIs) were selected from each video recording and the summation of contraction frequency and amplitude was denoted as gray value using the Multi Plot function (Image J). All measurements were made from three 10-minute recordings per mouse and 3–5 mice were analyzed per group.

Measurement of small intestinal transit

A 150 μl solution of 6% w/v carmine red in 0.5% methylcellulose was orally gavaged into the stomachs of WT and KO mice through a 21-gauge round-tip feeding needle. Food was withdrawn two hours before gavaging. Mice were sacrificed after 20 or 40 minutes. Small intestines were dissected and laid out, and the length of the tissue travelled by the carmine red dye was measured as a proportion of the total length of the small intestine. The assay was performed in n=4–6 mice per group, per time-point, and included both male and female mice within each group without any bias.

Measurement of gastric emptying

A 150 μl solution of 6% w/v carmine red in 0.5% methylcellulose was orally gavaged into the stomachs of *Ednrb* WT and KO mice through a 21-gauge round-tip feeding needle. Food was withdrawn two hours before gavaging. Mice were sacrificed after 20 minutes and stomachs were collected. Weight of the stomach before and after removing the stomach contents was recorded. Gastric emptying was calculated as the weight of contents emptied from the stomach as a proportion of the initial weight of the stomach. The assay was performed in n=4–5 mice per group and included both male and female mice within each group without any bias.

Statistical analysis

Values are typically represented as mean ± SEM (standard error of mean). Statistical analysis was performed using Prism 8 (GraphPad software, Inc., La Jolla, CA, USA).

Statistical significance between WT and KO mice was assessed using Student’s t-test. pvalues <0.05 were regarded significant.

3. Results

We examined the overall ENS architecture and function of the ganglionated bowel of mice with HSCR, focusing on the proximal colon, distal small intestine, and stomach. All studies were performed in $Ednrb^{-/-}$ (KO) mice, with $Ednrb^{+/+}$ (WT) littermates as controls. KO mice had distal colonic aganglionosis extending for about 1.5 cm in length, and this was confirmed by immunostaining with neuronal markers, Hu and Tuj1 (data not shown). Since

they generally survive only to about 4 weeks of age due to development of enterocolitis, all studies were performed in 3-week-old mice.

To characterize the ENS architecture of the proximal colon, cross sections of the colon were immunostained with the neuronal marker, Hu, and the glial/progenitor marker, Nestin, to label the myenteric ganglia (Fig 1a,b). Enteric ganglia size and number were analyzed. Although the number of ganglia per high-power field (HPF) in the proximal colon was similar in WT and KO mice (Fig 1c), ganglia were 56% smaller in size in the KO group (Fig 1d). Wholemount immunohistochemistry was performed on LMMP preparations from WT and KO proximal colon (Fig 1e,f). Enteric neuronal density (Fig. 1g) was calculated by counting Hu+ neuronal cell bodies per HPF and was found to be 36% lower in KO mice as compared to WT, although this did not reach statistical significance. Neuronal fiber density (Fig. 1h) was significantly lower in KO mice. Packing density, which reflects the number of neuronal cell bodies per area of myenteric ganglia, was similar between the two groups (Fig 1i).

To functionally characterize the proximal colon of KO mice, spatiotemporal mapping was performed on explanted guts to examine colonic migrating motor complexes (CMMCs). These represent neurally-mediated, rhythmic, spontaneous propagating contractions in the mouse colon. Kymographs of intestinal diameter changes as a measure of gut contractility were generated from 30-minute video recordings. In WT mice, 3.6 ± 0.6 CMMCs (Fig 2a, arrows) were observed over a 10-minute recording. The average distance covered by the CMMCs was 12.8 ± 2.1 mm, with a velocity of 0.6 ± 0.4 mm/s. These coordinated contraction patterns were markedly decreased, and nearly absent, in the proximal colon of all KO mice examined (Fig 2b,c).

ENS architecture in the distal small intestine was analyzed in cross sections immunostained with the neuronal antibody, Hu (Fig 3a,b). KO mice had a significantly lower enteric ganglia density as compared to WT (Fig 3c). Ganglion size was similar between the two groups (Fig 3d). Immunofluorescence of LMMP wholemount preparations from the distal small intestine (Fig 3e, 3f) showed that neuronal cell body density was similar between WT and KO mice (Fig 3g), while KO mice exhibited significantly lower neuronal fiber density (Fig 3h). Neuronal cells were also found to be more densely packed in the small intestinal myenteric ganglia in KO mice (Fig 3i). This is consistent with the observation that despite having fewer ganglia per area (Fig. 3c), KO animals have equivalent neuronal numbers per HPF (Fig. 3g).

Small intestinal motility was compared using both spatiotemporal mapping and intestinal transit time. Non-propagating segmentation contractions in WT and KO mice were examined *ex vivo* and kymographs generated to quantify contraction frequency and amplitude in the two groups (Fig 4a, 4b). The area under the curve (AUC) was used to represent the summation of contractile activities over a given period of time (Fig 4c). No significant difference between KO and WT was seen in the frequency (31.9 ± 4.1 in WT vs 31.9 ± 2.6 in KO; Fig 4d), maximum amplitude (175.2 ± 1.6 in WT vs 174.6 ± 6.8 in KO; Fig 4e) or AUC (3744 ± 56 in WT vs 3663 ± 77.2 in KO; Fig 4f).

To assess transit time, mice were gavaged with non-absorbable carmine red dye and the percentage of the total small intestine traversed by the dye was recorded at 20- and 40minutes post-gavage. There was no difference in small intestinal transit at 20 minutes (43.9 ± 4.1% in n=5 WT vs 46.9 ± 10.6% in n=4 KO). At 40 minutes, however, small intestinal transit was significantly delayed by 26% in KO mice (66.3 ± 4.4% in n=6 WT vs 48.9 ± 2.8% in n=4 KO; Fig 4g), suggesting a delay in the distal half of the small intestine.

Finally, ENS structure and function were characterized in the gastric antrum. LMMP preparations from the stomach of WT and KO mice were immunostained with Hu and Tuj1 (Fig 5a, 5b). Density of neuronal cell bodies and fibers was quantitatively compared and found to be similar in the two groups (Fig 5c,d). Interestingly, neuronal packing density was markedly higher in KO stomachs (Fig 5e), similar to the changes seen in the small intestine. To determine whether gastric function is altered, we measured gastric emptying in these mice and found that KO mice had significantly faster gastric emptying as compared to controls (77.95 ± 3.2% in WT vs 94.78 ± 0.7% in KO). Findings from stomach, small intestine, and colon are summarized in Table 1.

4. Discussion

Resection of aganglionic bowel is lifesaving for infants with HSCR, but follow-up studies have found that many patients continue to suffer from long-term functional bowel abnormalities after pullthrough surgery [17–20]. Moreover, manometry and imaging studies have suggested the presence of altered contractility and transit throughout the GI tract in HSCR patients, including in the esophagus, stomach, duodenum, and colon [610]. This suggests that ENS abnormalities may extend well beyond the aganglionic segment and transition zone, which has major implications for how we evaluate and treat patients with post-pullthrough GI morbidity. In this study, we report on ENS morphology and GI function in the proximal colon, small intestine, and stomach in the *Ednrb* KO mouse model of HSCR. Our findings extend observations made in prior studies, showing structural ENS abnormalities and functional alterations in motility and transit extending from the stomach to the colon.

While the transition zone proximal to the aganglionic segment is known to be associated with poor motility, we found a complete absence of CMMCs in the proximal colon of HSCR mice, well above the transitional segment. Complete loss of CMMCs throughout the colon has previously been reported in *Gdnf*$^{+/-}$ mice and *Et3*$^{-/-}$ mice [21], which are models of hypoganglionosis and distal aganglionosis, respectively. Loss of CMMCs in our *Ednrb* KO model correlated with structural abnormalities of the ENS, including smaller myenteric ganglia and lower neuronal fiber density. These changes were seen in the most proximal part of the colon, despite the fact that the aganglionosis affects only the most distal colon. A hypoganglionic phenotype of the proximal colon similar to our findings has been previously reported in other HSCR models. For example, one study demonstrated a decreased density of myenteric ganglia along the entire length of the colon in a model of HSCR caused be a spontaneous deletion of the *Ednrb* gene [22]. Similarly, the ganglionated colon of mice harboring a neural crest cell-specific deletion of the *Ednrb* gene have smaller and sparser ganglia, along with larger neuronal cell bodies [11]. Along with the present study, these

findings suggest that HSCR may be associated with alterations of ENS structure and function in proximal colon remote from the aganglionic zone, a region often presumed to be normal. As many HSCR patients suffer from persistent constipation and obstructive symptoms after pullthrough surgery, it will be important to understand how these subtle changes in ENS morphology affect function. These symptoms of persistent obstruction may be partially due to postoperative sphincter dysfunction, but our results suggest that neuronal abnormalities may also contribute.

Interestingly, ENS structural differences were also identified in the small intestine, where *Ednrb* KO mice had a significantly reduced density of myenteric ganglia and neuronal fibers and an associated delay in *in vivo* small intestinal transit, but not in *ex vivo* spatiotemporal maps. Spatiotemporal mapping of small intestinal contractions was performed in non-fasted mice. Our kymographs showed short, rhythmic, motor contraction patterns characteristic of segmentation, which has both myogenic and neurogenic components. There was no difference in small intestinal contractions between WT and KO mice. Interestingly, recent reports have shown that segmentation contractions can occur in the presence of nerve conduction blockade [23], and therefore these contractions can be preserved even in the setting of an abnormal ENS. We therefore hypothesize that the hypoganglionosis we observed in KO mice might not directly affect segmentation patterns and that is why we observe no difference in the spatiotemporal maps. In contrast, small intestinal transit is more complex and reflects the relative contributions of receptive relaxation, segmentation, peristalsis, and retropropulsion [24]. Since the *in vivo* assay for measurement of small intestinal transit was performed in a fasted state, motor activity is likely being impacted by interdigestive migrating motor complexes, and less so by segmentation, which occurs predominantly in a non-fasted gut. The exact contribution of the ENS in controlling this aspect of motility is not fully understood. These proximal ENS and transit abnormalities correlate with prior studies in HSCR patients. One study showed that 3 of 12 patients with either HSCR or intestinal hypoganglionosis had delayed transit of barium from the stomach to the colon [6]. Another paper reports that 12 of 12 children with total colonic aganglionosis had manometric abnormalities present in the esophagus and duodenum [7]. We identified smaller ganglia in the proximal colon and fewer ganglia in the distal small intestine, both of which are consistent with hypoganglionosis. It is unclear why the phenotype of hypoganglionosis differs between the small and large intestine. The molecular determinants of ganglion size versus ganglion number during ENS development are not known. One hypothesis that could explain the development of small ganglia is based on data from Rollo et al [25], who showed that neurons are highly adhesive and drive core ganglion formation, while non-neuronal cells accumulate on the outer surface of the ganglion and are non-adhesive. Loss of Ednrb signaling decreases neuronal numbers in the colon and this may explain the smaller core ganglion size in the proximal colon. Why ganglion number, rather than size, is reduced in the small intestine is unknown. Overall, our results imply diffuse ENS abnormalities throughout the large and small intestine in HSCR.

We found structural and functional abnormalities extending proximally to the stomach in our study, with KO mice displaying altered ENS structure in the stomach and accelerated gastric emptying. Gastric emptying has been variably described as accelerated or delayed in HSCR. Miele and colleagues reported that children with HSCR, at an average of 6.6 years after

surgery, retain radiotracer-labeled solid food in their stomach significantly longer than healthy, age-matched control children [9]. Similarly, Medhus et al identified a decreased rate of gastric emptying of both liquids and solids as measured by radiotracer analysis in young adult HSCR patients compared with controls, although the control subjects were on average 5 years older than the HSCR patients [10]. Clinical data also suggests association of HSCR with gastroesophageal reflux in some patients [26]. Conversely, there is a report of a patient with Haddad syndrome who passed barium from the mouth to a transverse colostomy in under 30 minutes and subsequently experienced dumping syndrome [27], consistent with accelerated gastric emptying. Increased gastric emptying has also been described in *Sox10*$^{Dom/+}$ HSCR mice [28]. We speculate that specific HSCR mutations and resulting ENS abnormalities may predispose to either delayed or accelerated gastric emptying. Interspecies differences may also account for this apparent discrepancy. Regardless, both our data and experience with human patients suggests the presence of some degree of upper GI dysmotility in HSCR patients. Further work is necessary to determine whether structural and/or functional alterations in the upper GI tract are a general feature of HSCR and to understand their etiology and implications.

We conclude that HSCR encompasses more than distal colonic aganglionosis. The evidence suggests that HSCR may represent a pan-gastrointestinal disease with both structural and functional consequences that can extend from the esophagus to the colon. Further studies are needed to determine whether these abnormalities are specific to HSCR patients with an *Ednrb* mutation or are a general feature of all HSCR cases. This study has important implications for the evaluation and diagnosis of patients experiencing GI morbidity following pullthrough surgery and may help us to improve their management.

Acknowledgments

Funding sources:

AMG is supported by the National Institutes of Health (R01DK103785).

Abbreviations

HSCR	Hirschsprung disease
GI	Gastrointestinal
ENS	Enteric nervous system
WT	Wildtype
KO	Knockout
LMMP	Longitudinal muscle myenteric plexus
GIMM	Gastrointestinal motility monitor
CMMC	Colonic migrating motor complex
AUC	Area under the curve

ROI	Region of interest
HPF	High-power field

References

[1]. Goldstein AM, Thapar N, Karunaratne TB, De Giorgio R. Clinical aspects of neurointestinal disease: Pathophysiology, diagnosis, and treatment. Dev Biol 2016;417(2):217–28. [PubMed: 27059882]

[2]. Goldstein AM, Hofstra RM, Burns AJ. Building a brain in the gut: development of the enteric nervous system. Clin Genet 2013;83(4):307–16. [PubMed: 23167617]

[3]. Anderson JE, Vanover MA, Saadai P, Stark RA, Stephenson JT, Hirose S. Epidemiology of Hirschsprung disease in California from 1995 to 2013. Pediatr Surg Int 2018;34(12):1299–303. [PubMed: 30324568]

[4]. Yanchar NL, Soucy P. Long-term outcome after Hirschsprung's disease: patients' perspectives. J Pediatr Surg 1999;34(7):1152–60. [PubMed: 10442612]

[5]. Widyasari A, Pravitasari WA, Dwihantoro A, Gunadi. Functional outcomes in Hirschsprung disease patients after transabdominal Soave and Duhamel procedures. BMC gastroenterology 2018;18(1):56. [PubMed: 29703156]

[6]. Tomita R, Ikeda T, Fujisaki S, Shibata M, Tanjih K. Upper gut motility of Hirschsprung's disease and its allied disorders in adults. Hepatogastroenterology 2003;50(54):1959–62. [PubMed: 14696442]

[7]. Faure C, Ategbo S, Ferreira GC, Cargill G, Bellaiche M, Boige N, Viarme F, Aigrain Y, Cezard JP, Navarro J. Duodenal and esophageal manometry in total colonic aganglionosis. J Pediatr Gastroenterol Nutr 1994;18(2):193–9. [PubMed: 8014767]

[8]. Staiano A, Corazziari E, Andreotti MR, Clouse RE. Esophageal motility in children with Hirschsprung's disease. American journal of diseases of children (1960) 1991;145(3):310–3. [PubMed: 2003481]

[9]. Miele E, Tozzi A, Staiano A, Toraldo C, Esposito C, Clouse RE. Persistence of abnormal gastrointestinal motility after operation for Hirschsprung's disease. Am J Gastroenterol 2000;95(5):1226–30. [PubMed: 10811332]

[10]. Medhus AW, Bjornland K, Emblem R, Husebye E. Liquid and solid gastric emptying in adults treated for Hirschsprung's disease during early childhood. Scand J Gastroenterol 2007;42(1):34–40. [PubMed: 17190760]

[11]. Zaitoun I, Erickson CS, Barlow AJ, Klein TR, Heneghan AF, Pierre JF, Epstein ML, Gosain A. Altered neuronal density and neurotransmitter expression in the ganglionated region of Ednrb null mice: implications for Hirschsprung's disease. Neurogastroenterol Motil 2013;25(3):e233–44. [PubMed: 23360229]

[12]. Cheng LS, Schwartz DM, Hotta R, Graham HK, Goldstein AM. Bowel dysfunction following pullthrough surgery is associated with an overabundance of nitrergic neurons in Hirschsprung disease. J Pediatr Surg 2016;51(11):1834–8. [PubMed: 27570241]

[13]. Hosoda K, Hammer RE, Richardson JA, Baynash AG, Cheung JC, Giaid A, Yanagisawa M. Targeted and natural (piebald-lethal) mutations of endothelin-B receptor gene produce megacolon associated with spotted coat color in mice. Cell 1994;79(7):1267–76. [PubMed: 8001159]

[14]. Thiagarajah JR, Yildiz H, Carlson T, Thomas AR, Steiger C, Pieretti A, Zukerberg LR, Carrier RL, Goldstein AM. Altered goblet cell differentiation and surface mucus properties in Hirschsprung disease. PLoS One 2014;9(6):e99944. [PubMed: 24945437]

[15]. Hoffman JM, Brooks EM, Mawe GM. Gastrointestinal Motility Monitor (GIMM). J Vis Exp 2010(46).

[16]. Barnes KJ, Spencer NJ. Can colonic migrating motor complexes occur in mice lacking the endothelin-3 gene? Clin Exp Pharmacol Physiol 2015;42(5):48595.

[17]. Rintala RJ, Pakarinen MP. Long-term outcomes of Hirschsprung's disease. Semin Pediatr Surg 2012;21(4):336–43. [PubMed: 22985839]

[18]. Neuvonen MI, Kyrklund K, Rintala RJ, Pakarinen MP. Bowel Function and Quality of Life After Transanal Endorectal Pull-through for Hirschsprung Disease: Controlled Outcomes up to Adulthood. Ann Surg 2017;265(3):622–9. [PubMed: 28169931]

[19]. Kyrklund K, Neuvonen MI, Pakarinen MP, Rintala RJ. Social Morbidity in Relation to Bowel Functional Outcomes and Quality of Life in Anorectal Malformations and Hirschsprung's Disease. Eur J Pediatr Surg 2018;28(6):522–8. [PubMed: 29059696]

[20]. Granstrom AL, Danielson J, Husberg B, Nordenskjold A, Wester T. Adult outcomes after surgery for Hirschsprung's disease: Evaluation of bowel function and quality of life. J Pediatr Surg 2015;50(11):1865–9. [PubMed: 26164226]

[21]. Roberts RR, Bornstein JC, Bergner AJ, Young HM. Disturbances of colonic motility in mouse models of Hirschsprung's disease. Am J Physiol Gastrointest Liver Physiol 2008;294(4):G996–G1008. [PubMed: 18276829]

[22]. Ro S, Hwang SJ, Muto M, Jewett WK, Spencer NJ. Anatomic modifications in the enteric nervous system of piebald mice and physiological consequences to colonic motor activity. Am J Physiol Gastrointest Liver Physiol 2006;290(4):G710–8. [PubMed: 16339294]

[23]. Huizinga JD, Chen JH. The myogenic and neurogenic components of the rhythmic segmentation motor patterns of the intestine. Frontiers in neuroscience 2014;8:78. [PubMed: 24782705]

[24]. Bornstein JC. Purinergic mechanisms in the control of gastrointestinal motility. Purinergic Signal 2008;4(3):197–212. [PubMed: 18368521]

[25]. Rollo BN, Zhang D, Simkin JE, Menheniott TR, Newgreen DF. Why are enteric ganglia so small? Role of differential adhesion of enteric neurons and enteric neural crest cells. F1000Res 2015;4:113. [PubMed: 26064478]

[26]. Rogers M, Ammoury R. Hirschsprung's Disease Causing Constipation in an Infant. ACG Case Rep J 2016;3(4):e126. [PubMed: 27807578]

[27]. Rivkees SA, Crawford JD. Hypoglycemia pathogenesis in children with dumping syndrome. Pediatrics 1987;80(6):937–42. [PubMed: 3317264]

[28]. Musser MA, Correa H, Southard-Smith EM. Enteric neuron imbalance and proximal dysmotility in ganglionated intestine of the Sox10Dom/+ Hirschsprung mouse model. Cell Mol Gastroenterol Hepatol 2015;1(1):87–101. [PubMed: 25844395]

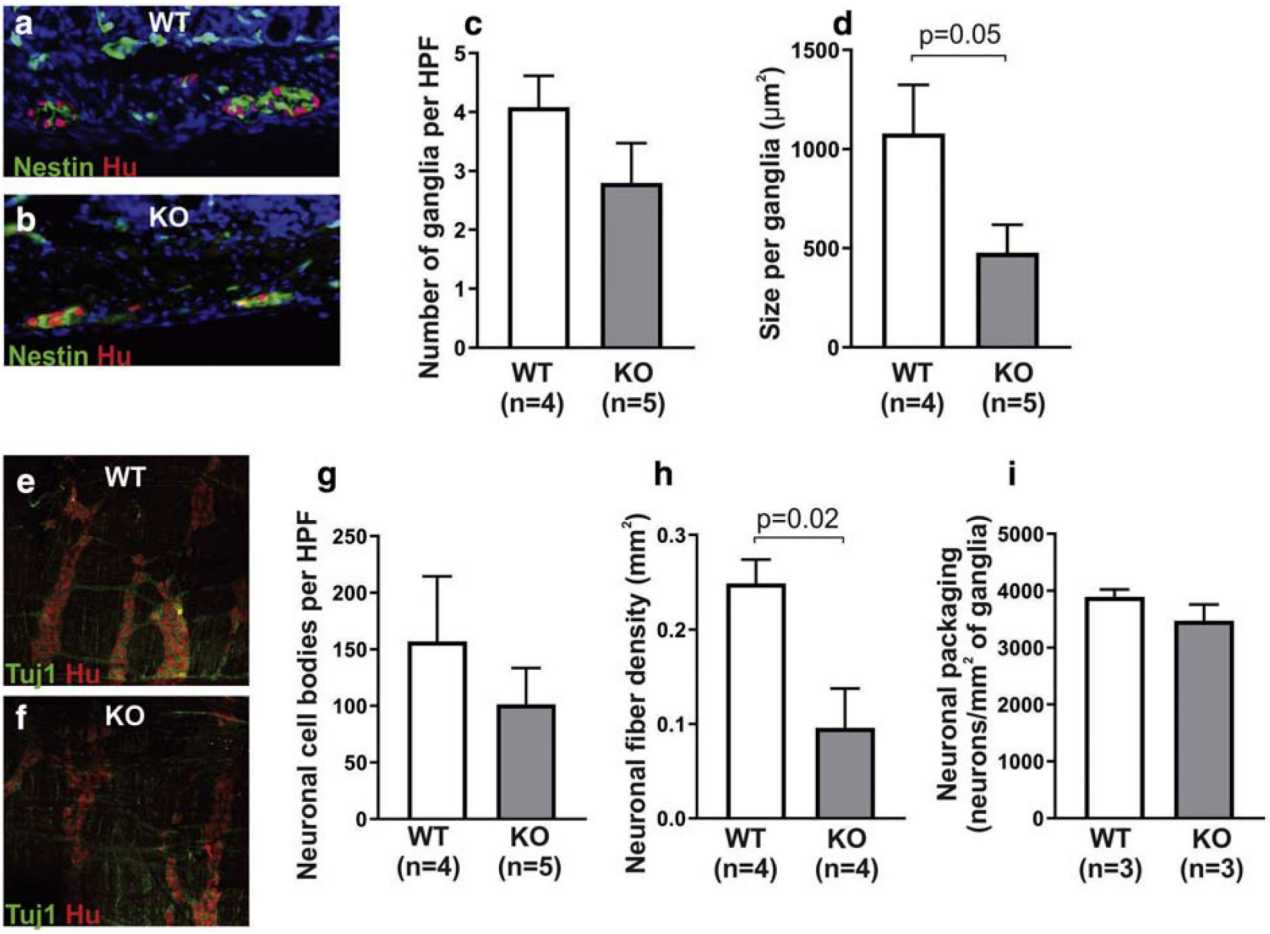

Figure 1. ***Ednrb*** **KO mice possess ENS abnormalities in the ganglionated proximal colon.**

Cross sections of the colon were stained with neuronal (Hu) and glial (Nestin) antibodies (a,b) and show that KO mice have a similar density of ganglia (c), but the ganglia are smaller in size (d). Wholemount preparations stained with neuronal antibodies, Tuj1 and Hu (e, f), reveal that neuronal cell density in the myenteric plexus is similar between the two groups (g), but KO mice have lower nerve fiber density (h). No difference in neuronal packing density was seen between the two groups (i).

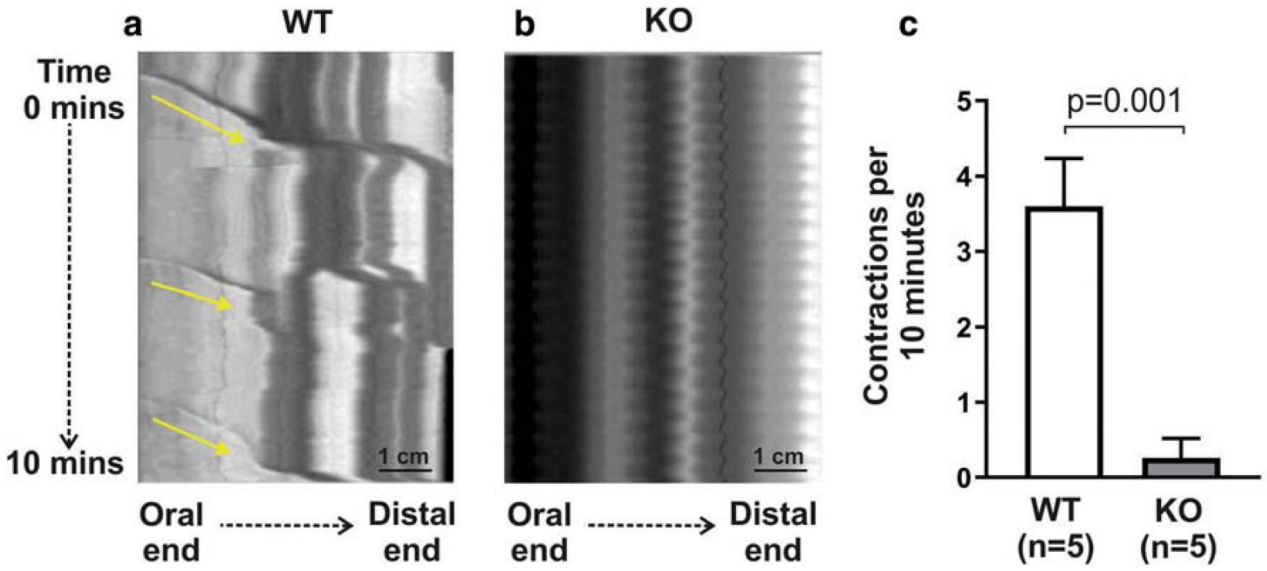

Figure 2. Proximal colon of *Ednrb* KO mice has markedly abnormal contractile function.

Spatiotemporal mapping of colonic contractility shows normal propagating CMMCs in WT mice (a, arrows), but these are nearly absent in KO (b,c).

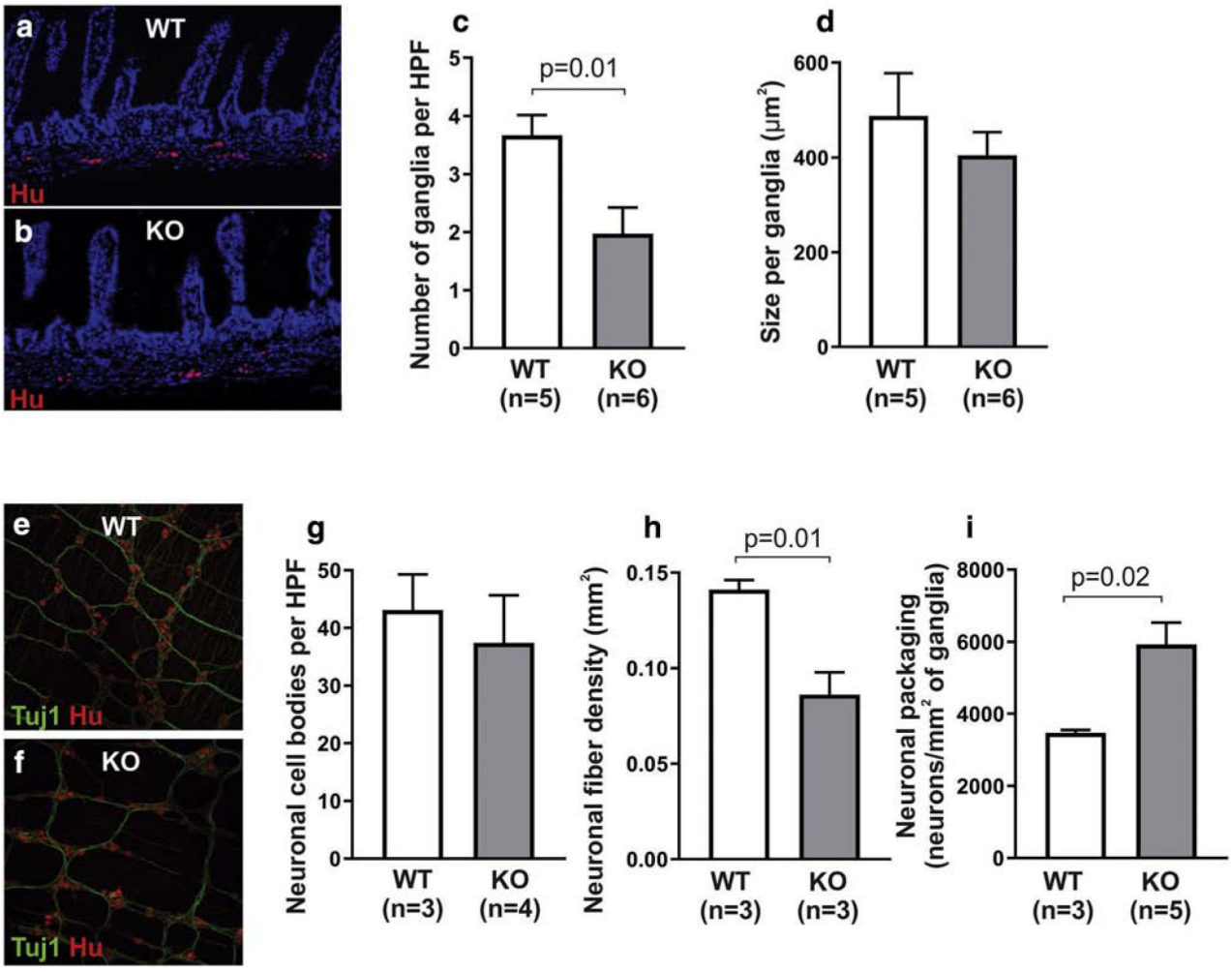

Figure 3. ENS abnormalities are present in the distal small intestine of *Ednrb* KO.

Cross sections of the small intestine were stained with the neuronal antibody, Hu (a,b), and reveal lower ganglion density in KO mice (c), but with similar ganglion size (d). Wholemount preparations stained with neuronal antibodies, Tuj1 and Hu (e, f), show that neuronal cell density in the myenteric plexus is similar between the two groups (g), but KO mice have lower nerve fiber density (h) and increased neuronal packing density (i).

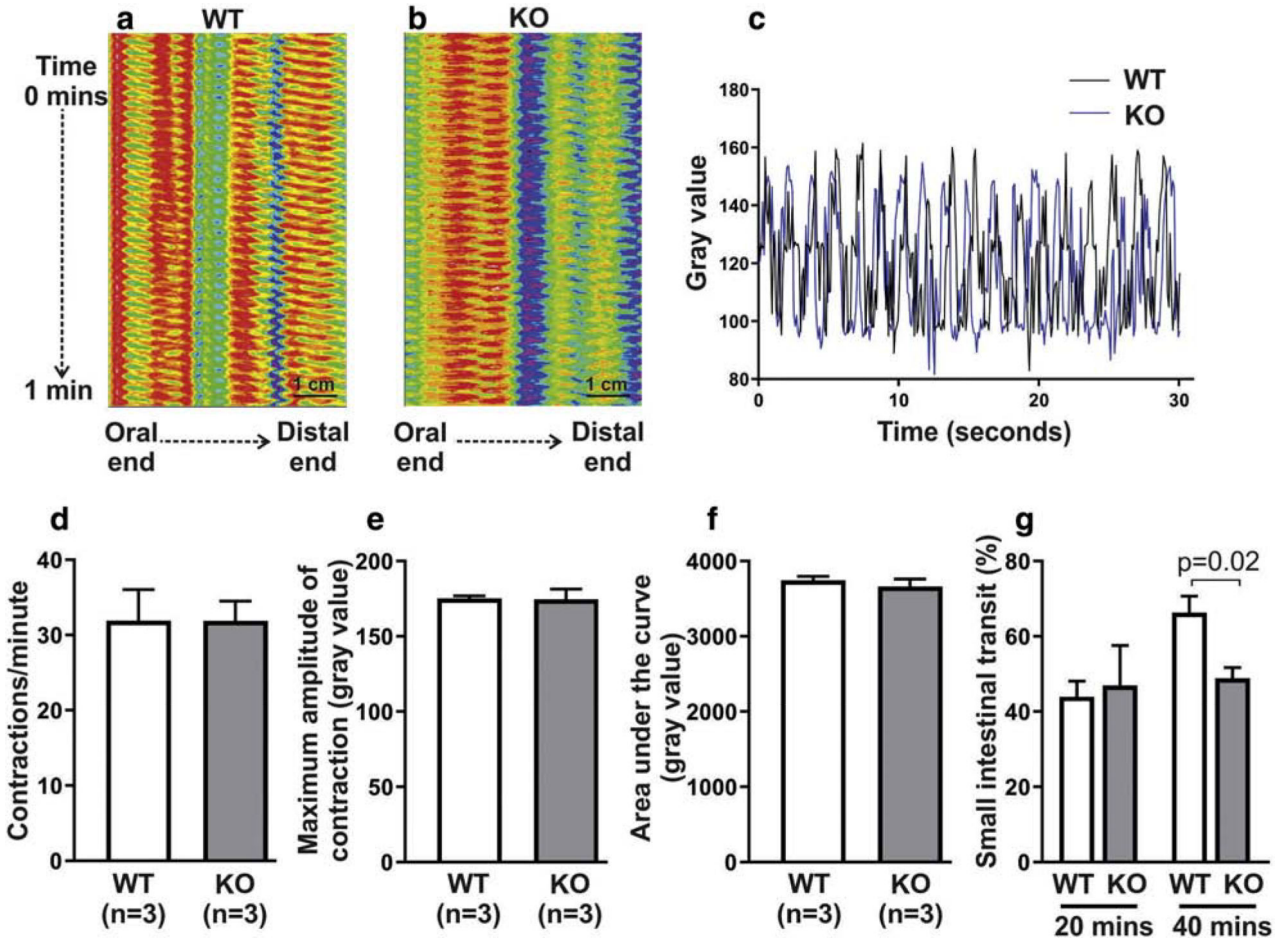

Figure 4. Distal small intestinal transit is delayed in *Ednrb* KO mice.

Spatiotemporal mapping of distal small intestine (a-c) shows that the frequency (d), amplitude (e), and AUC (f) of segmentation contractions are not altered in *Ednrb* KO mice. *In vivo* analysis of intestinal transit, however, shows a significant delay at 40 minutes, but not 20 minutes, in KO mice (g), corresponding with delayed transit in the distal half of the small intestine.

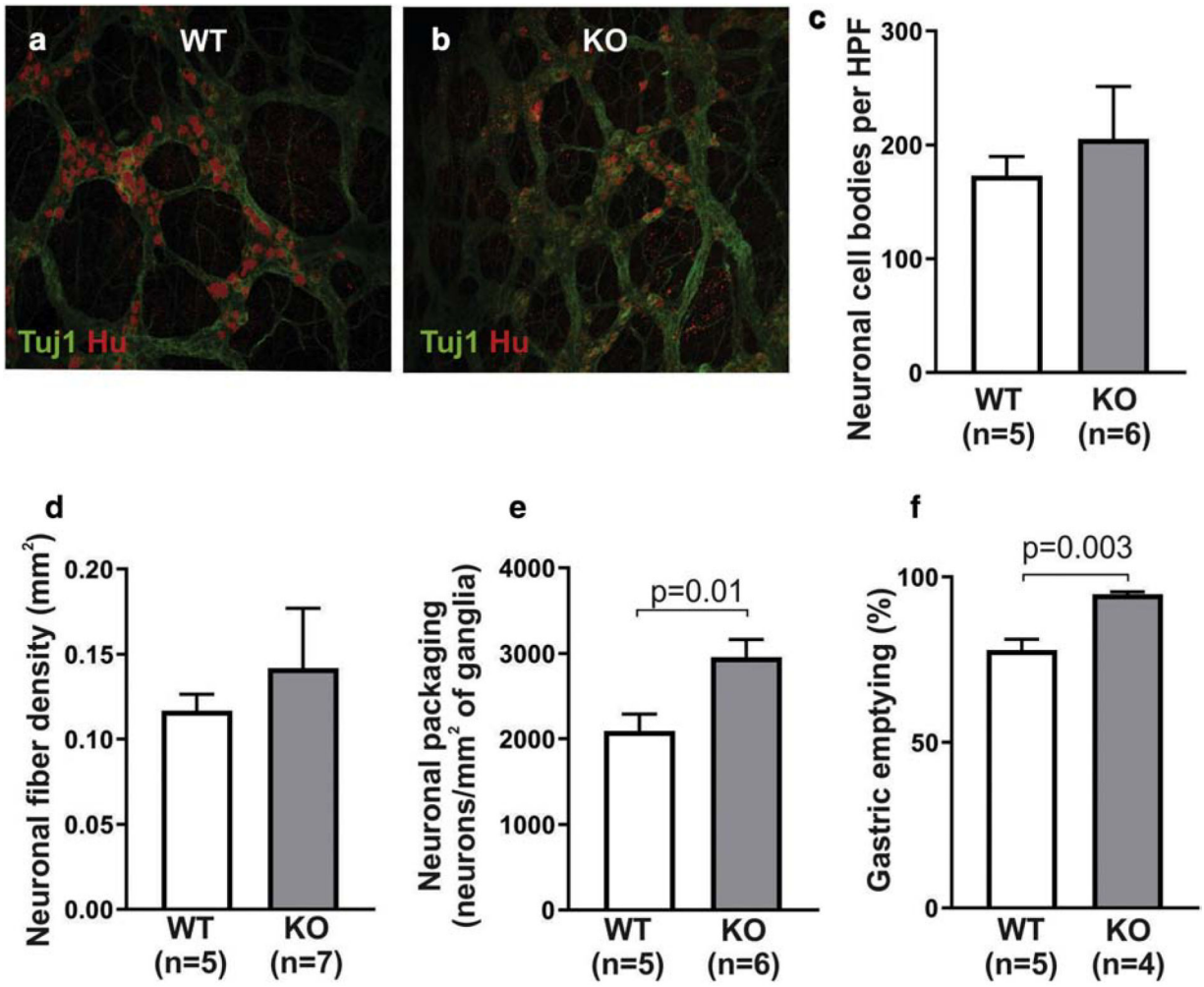

Figure 5. *Ednrb* KO mice exhibit ENS abnormalities and motor dysfunction in the gastric antrum.

Wholemount preparations of gastric myenteric plexus were stained with neuronal antibodies, Tuj1 and Hu (a, b). Quantitative analysis demonstrates similar density of neuronal cell bodies (c) and neuronal fibers (d) between the two groups, with a higher neuronal packing density in KO mice (e). Gastric emptying was significantly faster in the KO group (f).

Table 1.

Summary of structural ENS anomalies and motor dysfunction in *Ednrb* KO mice as compared to WT littermates.

	Number of ganglia per field	Size per ganglia	Neuronal cell bodies per field	Neuronal fiber density	Neuronal packing density	GI function
Proximal Colon	ND	↓	ND	↓	ND	↓
Distal Small Intestine	↓	ND	ND	↓	↑	↓
Stomach	–	–	ND	ND	↑	↑

ND: no difference